A Novel Method for the Use of Carrier Smoothing in the Loosely Coupled GPS/INS Integration

Thuan D. Nguyen*, Tung H. Ta, Vinh T. La, Lan T. H. Nguyen
Hanoi University of Science and Technology, No. 1, Dai Co Viet, Hai Ba Trung, Hanoi, Viet Nam
Received: September 08, 2016; accepted: June 9, 2017

Abstract

The performance of the loosely coupled GPS/INS integration (LC) can be improved by the use of carrier measurements. However, the existing solutions are mostly based on the Real Time Kinematic (RTK) technique which requires an expensive base station for corrections. In this paper, a LC architecture with carrier smoothing is proposed for the use of carrier pseudorange without that station. The proposed architecture is based on the fact that carrier pseudorange can be smoothed by the combination of code and carrier pseudorange. Owing to absence of the base station, it is expected that this approach can achieve better results than the traditional approach does. Evaluation results demonstrate that the error in position of the proposed architecture are smaller than that of traditional architecture up to several meters.

Keywords: GPS/INS, carrier smoothing, loosely coupled

1. Introduction

The GPS/INS integration has become an effective approach in multi-sensors integration. This is because GPS receivers and INS sensors can complement each other to achieve the greatest benefits of all. In more detail, INS sensors can provide the position and angles at a quicker update rate than GPS but their errors are increasingly over time due to the behavior of IMU sensors. In contrast, the GPS-based position is calculated independently for every epoch. Consequently, the GPS solution can be used to compensate the errors raised by INS sensors.

Amongst GPS/INS integration approaches, LC is the most common technique due to its simple implementation. Moreover, this technique requires the type of GPS data which can be provided by low-cost GPS receivers. Therefore, LC has been considered as a low-cost solution to GPS/INS integration. Although the performance of this technique degrades if equipped with low-cost receivers, it can be improved by using carrier measurements in PVT (Position-Velocity-Time) computation. Particularly, the PVT solution of GPS receivers can be estimated based on either GPS code phase or GPS carrier phase. The latter has a higher accuracy due to the smaller resolution than that of the code phase. Hence, if an ambiguous number of integer cycles in the carrier phase is solved, the PVT solution based on carrier pseudoranges can achieve the better result [1].

Recently, the applying carrier measurements to GPS/INS integration is relied on the RTK technique [2]. However, this algorithm requires a setup of a base station using a high-grade receiver. The rover uses the information of the base station to solve the integer ambiguity and correct the errors raised by GPS satellites, the receiver, and transmitting media [2]. In addition, data processing programs must be implemented on both base and rover. As a result, this solution not only increases the deployment cost but also increases the computational complexity.

Another solution to bring benefits from carrier measurements without the setup of the station is the carrier smoothing. This method reduces the noise buried in carrier pseudoranges. However, to the best of our knowledge, there is no existing study of the integration of GPS and INS with the use of this strategy. Hence, in this paper, we propose a method for the use of carrier smoothing in the GPS/INS integration. In addition, the performance evaluation of this model also fully reported in this paper.

The rest of the paper is organized as follows. Firstly, we introduce the traditional model of loosely coupled GPS/INS integration and the proposed model. Secondly, we evaluate the performance of the new model. Finally, we draw some conclusions and further work.

2. Proposed Model

Our proposed model is inherited from the traditional model. Therefore, it is worth to mention the traditional LC model and brief explanations of processing blocks in the beginning of this section.

2.1. Traditinal Model

The traditional technique applied to this integration is shown in Fig. 1. The architecture

* Corresponding author: Tel.: (+84) 966614396
Email: thuan.nguyendinh@hust.edu.vn

contains three processing blocks namely: mechanization equations, PVT computation, and INS Kalman filter. The first block, which is so-called INS mechanization, computes the user position and velocity from the IMU sensor outputs. The second block called PVT computation takes the GPS receiver output to compute PVT. The INS Kalman filter combines the outputs from those two blocks by applying the Kalman filter. The difference between the estimated and predicted position is fed forward to the mechanization equations in the next epoch.

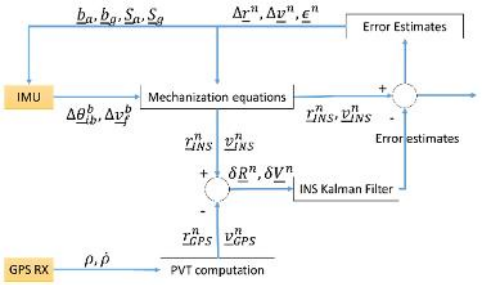

Fig. 1. Traditional loosely coupled GPS/INS integration

According to [3,4], the equations which is applied in INS Kalman Filter block in Fig. 1 can be expressed as follows:

Prediction Stage:

$$\hat{x}_{k+1}^{-} = \Phi_k x^{+} \tag{1}$$

$$P_{k+1}^{-} = \Phi_k P_k^{+} \Phi_k{}^T + Q_k \tag{2}$$

Update Stage:

$$K_{k+1} = P_{k+1}^{-} H_{k+1}^T (H_{k+1} P_{k+1}^{-} H_{k+1}^T + R_{k+1})^{-1} \tag{3}$$

$$\hat{x}_{k+1}^{+} = \hat{x}_{k+1}^{-} + K_{k+1}(z_{k+1} - H_{k+1}\hat{x}_{k+1}^{-}) \tag{4}$$

$$P_{k+1}^{+} = (I - K_{k+1} H_{k+1}) P_{k+1}^{-} \tag{5}$$

where x is the state vector which is defined as follows:

$$x = \begin{bmatrix} \delta r^n & \delta v^n & \epsilon^n \end{bmatrix}^T \tag{6}$$

where δr^n, δv^n, and ϵ^n are the position errors, the velocity errors, and Euler angle errors of the estimate and the output of INS mechanization, respectively.

$$Q_k = \frac{1}{2}\left[\Phi_k G(t_k) Q(t_k) + G(t_k) Q(t_k) \Phi_k^T\right] \Delta t \tag{7}$$

In our system, the matrix Q is fixed as follows:

$$Q = \begin{bmatrix} diag(q_a) & 0_{3\times3} \\ 0_{3\times3} & diag(q_g) \end{bmatrix} \tag{8}$$

where q_a and q_g is the covariance noise of accelerometer, and gyroscope sensors. These quantities are calculated thank to Allan variance method [3].

$$G(t_k) = \begin{bmatrix} 0_{3\times3} & 0_{3\times3} \\ R_b^n(t_k) & 0_{3\times3} \\ 0_{3\times3} & R_b^n(t_k) \end{bmatrix} \tag{9}$$

The measurement vector is follows:

$$z = \begin{bmatrix} \delta R^n \\ \delta V^n \end{bmatrix} = \begin{bmatrix} r_{INS}^n - r_{GPS}^n \\ v_{INS}^n - v_{GPS}^n \end{bmatrix} = \begin{bmatrix} \varphi_{INS} - \varphi_{GPS} \\ \lambda_{INS} - \lambda_{GPS} \\ h_{INS} - h_{GPS} \\ v_{INS} - v_{GPS} \end{bmatrix}$$

Since φ and λ are are very small, we should multiply the first two rows of Equation (19) by $(R_M + h)$ and $(R_N + h)\cos\varphi$ to prevent the big error in the solution of this Kalman filter [5]:

$$z = \begin{bmatrix} \varphi_{INS} - \varphi_{GPS} \\ \lambda_{INS} - \lambda_{GPS} \\ h_{INS} - h_{GPS} \\ v_{INS} - v_{GPS} \end{bmatrix} \tag{10}$$

where φ_I, and φ_G are the latitude estimated by INS and GPS receiver, respectively. λ_I, and λ_G are the longitude estimated by INS and GPS, respectively. Similarly, h_I, and h_G are the height estimated by INS and GPS, respectively. v_I, and v_G are the velocity computed by INS and GPS, respectively. The radius of curvature R_M and the prime vertical R_N is given by:

$$R_M = \frac{a(1-e^2)}{(1-e^2\sin^2(\varphi))^{3/2}} \tag{11}$$

$$R_N = \frac{a}{(1-e^2\sin^2\varphi)^1/2} \tag{12}$$

where a = 6378317 meters and e = 0.0818.

The design matrix H can be written as follows:

$$H = \begin{bmatrix} R_M + h & 0 & 0 & 0 & 0 & 0 & 0_{1\times3} \\ 0 & (R_N + h)\cos\varphi & 0 & 0 & 0 & 0 & 0_{1\times3} \\ 0 & 0 & 1 & 0 & 0 & 0 & 0_{1\times3} \\ 0 & 0 & 1 & 0 & 0 & 0 & 0_{1\times3} \\ 0 & 0 & 0 & 1 & 0 & 0 & 0_{1\times3} \\ 0 & 0 & 0 & 0 & 1 & 0 & 0_{1\times3} \\ 0 & 0 & 0 & 0 & 0 & 1 & 0_{1\times3} \end{bmatrix} \tag{13}$$

The noise covariance matrix R at a certain coordinate is calculated as follows

$$H=\begin{bmatrix}(R_M+h)^2\sigma_{\varphi}^2 & 0 & 0 & 0 & 0 & 0\\ 0 & (R_N+h)^2\cos^2\varphi\,\sigma_{\lambda}^2 & 0 & 0 & 0 & 0\\ 0 & 0 & \sigma_h^2 & 0 & 0 & 0\\ 0 & 0 & 0 & \sigma_{V_N}^2 & 0 & 0\\ 0 & 0 & 0 & 0 & \sigma_{V_E}^2 & 0\\ 0 & 0 & 0 & 0 & 0 & \sigma_{V_D}^2\end{bmatrix} \quad (14)$$

The matrix Φ_k in the prediction state is given by:

$$\Phi_k = I + F(t_k)\Delta t + \frac{F(t_k)\Delta t^2}{2} \quad (16)$$

In (16), I is the identity matrix. The matrix F is described as follows:

$$F=\begin{bmatrix}F_{rr} & F_{rv} & 0_{3\times3}\\ F_{vr} & F_{vv} & (f^n\times)\\ F_{er} & F_{ev} & -(\omega_{in}^n\times)\end{bmatrix} \quad (17)$$

The component matrix of F is given by:

$$F=\begin{bmatrix}0 & 0 & -\frac{v_N}{(R_M+h)^2}\\ v_E\sin\Phi & 0 & -\frac{v_E}{(R_N+h)^2\cos\Phi}\\ 0 & 0 & -1\end{bmatrix} \quad (18)$$

$$F_{vr}=\begin{bmatrix}-2v_E\omega_E\cos\Phi-\frac{v_E^2}{(R_M+h)\cos^2\varphi} & 0 & -\frac{v_Nv_D}{(R_M+h)^2}+\frac{v_E^2\tan\varphi}{(R_N+h)^2}\\ -2\omega_E(v_N\cos\varphi-v_D\sin\varphi)+\frac{v_Ev_N}{(R_N+h)\cos^2\varphi} & 0 & -\frac{v_E(v_D+v_N\tan\varphi)}{(R_N+h)^2}\\ 2v_E\omega_E\sin\varphi & 0 & \frac{v_E^2}{(R_N+h)^2}+\frac{v_N^2}{(R_M+h)^2}-\frac{2g}{R_N+h}\end{bmatrix} \quad (19)$$

$$F_{vv}=\begin{bmatrix}\frac{v_D}{R_M+h} & -2\omega_E\sin\varphi-\frac{2v_E\tan\varphi}{R_N+h} & \frac{v_N}{R_M+h}\\ 2\omega_E\sin\varphi+\frac{v_e\tan\varphi}{R_N+h} & \frac{v_D+v_N\tan\varphi}{R_N+h} & 2\omega_E\cos\varphi+\frac{v_E}{R_N+h}\\ -\frac{2v_N}{R_M+h} & -2\omega_E\cos\varphi-\frac{2v_E}{R_N+h} & 0\end{bmatrix} \quad (20)$$

$$F_{er}=\begin{bmatrix}-\omega_E\sin\varphi & 0 & -\frac{v_E}{(R_N+h)^2}\\ 0 & 0 & -\frac{v_N}{(R_M+h)^2}\\ -\omega_E\cos\varphi+\frac{v_E}{(R_N+h)\cos\varphi} & 0 & \frac{v_E\tan\varphi}{(R_N+h)^2}\end{bmatrix} \quad (21)$$

$$F_{ev}=\begin{bmatrix}0 & \frac{1}{R_N+h} & 0\\ -\frac{1}{R_M+h} & 0 & 0\\ 0 & 0 & -1\end{bmatrix} \quad (22)$$

Regards to the INS mechanization, although we will not go further to this subject in this paper, this component should be mentioned in the beginning of this section. According to [3,4], the INS mechanization is described as follows (Fig. 2) The output of IMU sensors (i.e angular velocities and forces) is fed to IMU mechanization block. Applying the processing

chain shown in Fig. 2, we can compute the position and velocity vector of the vehicle mounted the IMU.

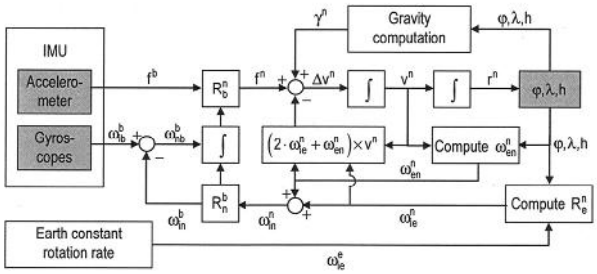

Fig. 2. INS mechanization [3].

In the LC strategy, the PVT can be either extracted from the used GPS receiver or computed using pseudoranges. In this paper, the second solution is chosen because it enables us to improve the PVT accuracy using advanced techniques. As shown in Fig. 2, the input of this block consists of pseudoranges and pseudorange-rates from every satellite in view. Amongst techniques used to compute PVT, least mean square error (LMS) is used due to the simplicity in implementation. This technique is also applied in our system. Due to the importance of this module, we would mention this block here in detail.

Considering the pseudorange measurement introduced by Misra and Enge [6,7]:

$$\rho^k(t) = r^k_{t,t-\tau} + c\Delta t_u(t) - c\Delta t^k(t-\tau) + I^k(t) + T^k(t) + \epsilon \quad (t) \quad (23)$$

where:

$\rho^k(t)$ is pseudorange measurement of the *k*th satellite (meters).

t is the signal reception time (seconds).

$r^k(t, t-\tau)$ is the geometric range between the receiver at the time reception, *t* and the *k*th satellite at the time of transmission, $t-\tau$ (meters).

τ is the time of flight (seconds).

c is the speed of light in a vacuum (meters/seconds).

$\delta t_u(t)$ is the receiver clock offset relative to GPS time at the signal at the time of reception (meters).

$\delta t^k(t-\tau)$ is the clock offset of the *k*th satellite to GPS time (meters).

$I^k(t)$ is the ionospheric delay of the *k*th satellite to GPS time (meters).

$T^k(t)$ is the propagation delay of the *k*th satellite (meters).

A LMS solution of (24) must satisfy the minimum expectation of $y-\epsilon$

$$y = h(x) + \epsilon \quad (24)$$

where ϵ is the white noise.

In PVT problem, *h(x)* and *x* at epoch *t* can be expressed as follows:

$$h(x) = \begin{bmatrix} r^1_{t,t-\tau} + c\Delta t_u(t) - c\Delta t^1(t-\tau) + I^1(t) + T^1(t) \\ r^2_{t,t-\tau} + c\Delta t_u(t) - c\Delta t^2(t-\tau) + I^2(t) + T^2(t) \\ \dots \\ r^M_{t,t-\tau} + c\Delta t_u(t) - c\Delta t^M(t-\tau) + I^M(t) + T^M(t) \end{bmatrix} \quad (25)$$

where M is the number of satellites in view.

An estimate of the user position is an convergence of (28). The process is initialized with an arbitrary value x_0

$$x = \begin{bmatrix} x_u \\ y_u \\ z_u \\ c\Delta t_u(t) \end{bmatrix} \quad (26)$$

$$\hat{x}_0 = x_0 \quad (27)$$

$$\hat{x}_{i+1} = \hat{x}_i + (H^T W H)^{-1} H^T W (y - h(\hat{x}_i)) \quad (28)$$

where H is the partial derivative matrix of $h(x)$ at $x = \hat{x}_i$. W is a weight matrix for the estimate.

2.2. Proposed model

The proposed model is shown in Fig. 3. In this model, we focus only on the PVT computation block. The proposed model of the PVT computation block is shown in Fig. 3. This block to smooth the pseudo-range is inserted to the between GPS receiver and PVT computation block. The remaining blocks are unchanged. Clearly, the proposed architecture minimizes the change of the overall system architecture.

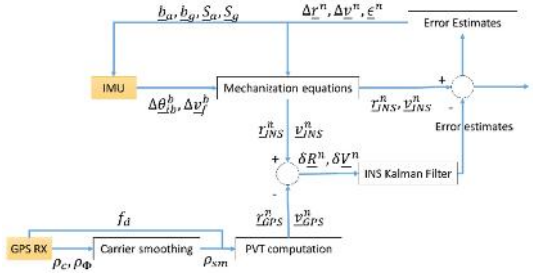

Fig. 3. Proposed LC with the use of carrier smoothing scheme

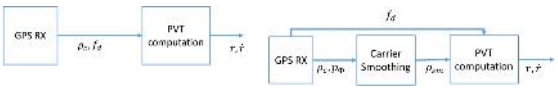

(a) (b)

Fig. 4. The traditional model (a) and the proposed model (b) of the PVT computation block

The computational chain of the smoothed pseudorange block is shown in Fig. 5.

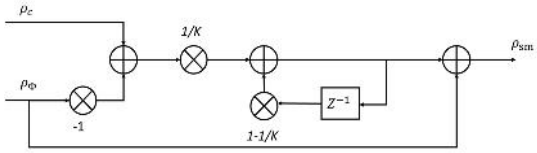

Fig. 5. Carrier smoothing diagram

It is straight forward to derive the following formula:

$$\tau_{sm}[n]=\frac{1}{K}\tau_{c}[n]+(1-\frac{1}{K})(\tau_{sm}[n-1]+\tau_{\Phi}[n]-\tau_{\Phi}[n-1]) \quad (29)$$

where $\rho_c[n]$, $\rho_\Phi[n]$, ρ_s $[n]$ are the code based pseudorange, the carrier phase based pseudorange, and the smoothed pseudorange, respectively. K is the weight factor of the estimate. By applying (29), it is proved that the output noise is reduced to 2K+1 times [8].

3. Results

In our experiments, the chosen IMU sensor and GPS receiver were 3DM-GX3 provided by MicroTrain and LEA-6P provided by Ublox, respectively (Fig. 6). The conducted experiments with two scenarios is described as belows.

Fig. 6. The experiment setup

In our experiment the GPS receiver and IMU are all mounted to a fixed frame and placed on the vehicle. The vehicle is then moved around the HUST campus following the trajectory illustrated in Fig. 7. In this mode, the position of every point in the reference trajectory is estimated using RTK technique. The base station is placed at a reference point in HUST. We verify the performance of the proposed model in both low DOP and high DOP cases. Therefore, we decide to choose 4 satellites following predefined scenarios as follows.

In the first case, the chosen satellites to compute PVT must satisfy the low DOP (Dilution Of Precision) value criteria (Fig. 8). The experiment lasts 250 seconds.

In the second case, the setup is the same as in the first case except for the chosen satellites for calculating PVT solution. In this case, the chosen satellites satisfy the high DOP value criteria (Fig. 10).

Fig. 7. The trajectory using in our experiment

3.1. The performance of the proposed model in a low-DOP condition

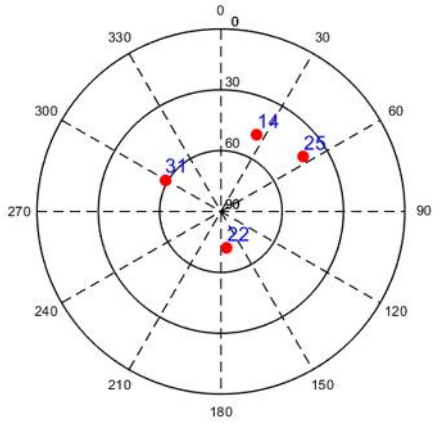

Fig. 8. Skyplot of the chosen satellites in the low DOP case

As shown in Fig. 9, the errors obtained by the proposed model are smaller than that of the traditional one. The estimated errors on all three directions for the proposed model is smaller than that of the traditional one from 1 to 1.5 meters. Table 1 shows the errors on average yielded by the experiment. Clearly, the error in the horizontal plane (i.e North and East direction) is much smaller than that of the vertical direction. This is because the used satellites are all above the receiver.

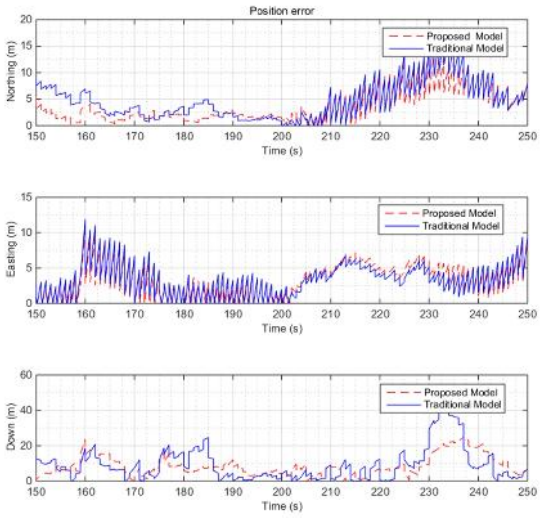

Fig. 9. Comparison between the proposed model w.r.t the traditional model in the low DOP case

Table 1. Performance comparison between the traditional LC model w.r.t the proposed model

	Proposed model (meters)	Traditional model (meters)
North	2.83	3.77
East	3.83	4.22
Down	8.90	10.44

3.2. The performance of the proposed model in a high-DOP condition

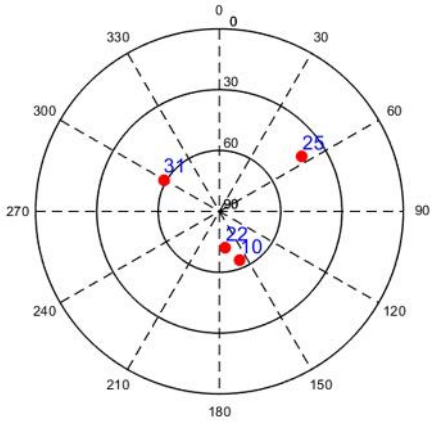

Fig. 10. Sky plot of satellites in view in the high DOP case

As illustrated in Fig. 11, the errors raised by the satellites configuration were much higher than that of the first case. This is because the distribution of the chosen satellites in this case are worse than that in the first case. In comparison the proposed w.r.t the traditional one, as expected, the obtained result is consistent with the first case which the proposed model has the better result.

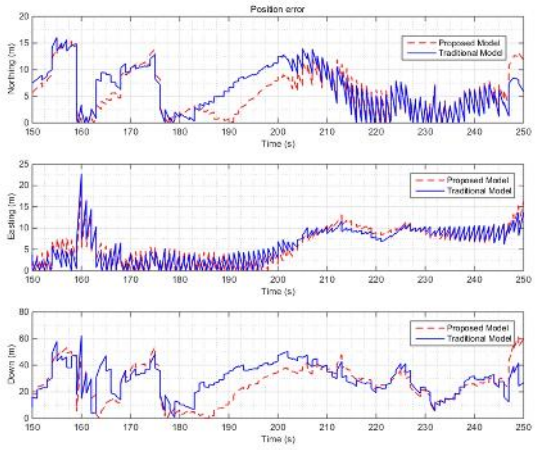

Fig. 11. Comparison between the proposed model w.r.t the traditional model in the high DOP case.

Table 2. Performance comparison between the traditional LC model w.r.t the proposed model

	Proposed model (meters)	Traditional model (meters)
North	5.57	6.37
East	5.99	5.82
Down	26.13	26.69

4. Conclusion

In this paper, we presented the new model of GPS/INS integration. In addition, the advantage of the new model was analyzed by comparing the performance of this model with the traditional one. Clearly, this model can be considered as an updated version of the traditional GPS/INS integration with the higher accuracy.

Acknowledgments

This work has been partially funded by the project B2013.01.47. We also would like to thank our colleges at the NAVIS Centre, Hanoi University Of Science and Technology, Vietnam because of their continuous help in our study. Besides providing the devices needed for our experiments, these colleges also give us valuable advices.

References

[1] Kaplan, Elliott, and Christopher Hegarty. Understanding GPS: principles and applications. Artech house, 2005.

[2] Stempfhuber, W., and M. Buchholz. "A precise, low-cost RTK GNSS system for UAV applications." Conference on Unmanned Aerial Vehicle in Geomatics, Zürich. 2011.

[3] Godha, Saurabh. Performance evaluation of low cost MEMS-based IMU integrated with GPS for land vehicle navigation application. Library and Archives Canada= Bibliothèque et Archives Canada, 2006.

[4] Shin, Eun-Hwan, and Naser El-Sheimy. Accuracy improvement of low cost INS/GPS for land applications. National Library of Canada= Bibliothèque nationale du Canada, 2003.

[5] Falco, Gianluca, et al. "Performance analysis of constrained loosely coupled GPS/INS integration solutions." Sensors 12.11 (2012): 15983-16007.

[6] Misra, Pratap, and Per Enge. Global Positioning System: Signals, Measurements and Performance Second Edition. Lincoln, MA: Ganga-Jamuna Press, 2006.

[7] Akos, Dennis, Alexandru Ene, and Jonas Thor. "A prototyping platform for multi-frequency GNSS receivers." ION GPS/GNSS Proceedings (2003).

[8] Presti, Lo. "Can you list all the properties of the carrier-smoothing filter?." INSIDE GNSS 10.4, (2015): 32-37.